1 **Formation of an Enduring Ensemble of Accumbens Neurons Leads to Prepotent Seeking**

2 **for Cocaine Over Natural Reward Cues**

3 Reda M Chalhoub[1,2,*], Anze Testen[1], Jordan Hopkins[1], Camille Carthy[1], and Peter W Kalivas[1,3]

4 [1] Department of Neuroscience, Medical University of South Carolina, Charleston, South Carolina, USA

5 [2] Medical Scientist Training Program, Medical University of South Carolina, Charleston, South Carolina,

6 USA

7 [3] Ralph Johnson Veterans Administration, Charleston, South Carolina, USA

8 [*] Corresponding Author and lead contact: chalhoub@musc.edu

9

10 SUMMARY

11 Neuronal activity in the nucleus accumbens core (NAcore) is necessary for reward-seeking

12 behaviors. We hypothesized that the differential encoding of natural and drug rewards in the

13 NAcore contributes to substance use disorder. We leveraged single-cell calcium imaging of

14 dopamine D1- and D2-receptor-expressing medium spiny neurons (MSNs) in the NAcore of mice

15 to examine differences between sucrose and cocaine rewarded (self-administration) and

16 unrewarded (abstinent and cue-induced) seeking. Activity was time-locked to nose-poking for

17 reward, clustered, and compared between sucrose and cocaine. Only in cocaine-trained mice were

18 excited D1-MSNs securely stable, capable of decoding nose-poking in all rewarded and

19 unrewarded sessions and correlated with the intensity of nose-poking for unrewarded seeking.

20 Furthermore, D1-MSNs formed a stable ensemble predictive of seeking behavior after extended

21 cocaine, but not sucrose abstinence. The excited D1-MSN ensemble uniquely drives cue-induced

22 cocaine seeking and may contribute to why drug seeking is prepotent over natural reward seeking

23 in cocaine use disorder.

26 INTRODUCTION

27 A major goal of research into the neural mechanisms of substance use disorder (SUD) is to

28 understand why a person suffering from SUD chooses to relapse to drug use at the expense of

29 engaging in nondrug rewarding life experiences. We hypothesized that an idea put forth over 30

30 years ago that discrete neuronal subpopulations within the brain, termed ensembles, encode

31 specific learned behaviors might offer insight into the underpinnings of this cardinal symptom of

32 SUDs[1]. The ensemble hypothesis has been invigorated over the last decade by advances in

33 visualizing and manipulating genetically discrete neuronal subgroups[2]. One approach uses

34 transgenic rodents transfected with immediate early gene (IEG) promoters that can mark neuronal

35 ensembles activated by initiating behaviors[3,4]. Also, advances in techniques to record the activity

36 of single neurons in freely behaving animals, including in-vivo electrophysiology[5,6] or single-cell

37 resolution calcium (Ca^{2+}) imaging[7,8], opened avenues for ensemble characterization.

38 In the field of SUDs research, the IEG approach reveals that drug seeking initiated by drug-

39 associated context and discrete cues requires activity in a relatively small ensemble of neurons (2-

40 3%) in the nucleus accumbens[4,9,10]. The nucleus accumbens is a well-established nexus in

41 processing both drug and natural reward seeking and is composed largely of two genetically

42 distinct subpopulations of medium spiny neurons expressing either D1 (D1-MSN) or D2 dopamine

43 receptors (D2-MSN)[11]. Importantly, the ensembles of IEG positive neurons induced by either

44 cocaine- or sucrose-conditioned cues overlap by only ~25%, indicating that the nucleus accumbens

45 uses largely separate ensembles to facilitate cue-initiated drug versus natural reward seeking[4], a

46 finding consistent with earlier in vivo electrophysiological measurements[12].

47 The IEG approach examines only neurons that are excited and does not consider neurons inhibited

48 by a stimulus, nor does it quantify time-specific changes in individual cell activity across task

49   performance[13]. For these reasons, we employed in vivo single cell Ca^{2+} imaging in male and female

50   mice expressing Cre recombinase in either D1- or D2-MSNs. We compared neuronal ensembles

51   created during cocaine or sucrose self-administration (rewarded seeking) and during two

52   unrewarded seeking sessions; after a period of abstinence and in response to reward-associated

53   cues after extinction training. This approach allowed us to record increases and decreases in

54   activity of accumbens D1- and D2-MSNs that were time-locked to a behavioral operand for

55   seeking behavior, active nose-pokes (NPs). Furthermore, we leveraged the spatial resolution of

56   calcium imaging to investigate and contrast the stability of recorded neurons over the time-course

57   of a single seeking session and longitudinally between seeking sessions.

58 RESULTS

59 ***Behavioral Responses:***

60 Mice were virally transfected with a Ca^{2+} reporter (pAAV-Syn-Flex-GCaMP6f-WPRE-SV40) into

61 the core subcompartment of the nucleus accumbens (NAcore) and 4-8 weeks later implanted with

62 a lens over the viral injection site (Figure 1a-c)[14]. Transfected neurons were visible in 26 of 35

63 mice, which were divided into two groups and trained for 12 days to self-administer either cocaine

64 or sucrose pellets paired with a light/tone cue (Figures 1d-f). During sucrose or cocaine self-

65 administration, active NPs were reinforced by a sucrose pellet or cocaine infusion when NPs were

66 separated by a 20 sec time-out period, while inactive NPs never delivered a reward. Following 10

67 days of forced abstinence, mice were returned to the operant chamber for a session with cues but

68 no reinforcer (termed post-abstinence seeking) to test for drug seeking, followed by 5-10 days of

69 extinction training to criterion without cue or reinforcer presentation. After extinction training was

70 completed, mice underwent cued reinstatement, during which active NPs by extinguished mice

71 yielded cue only. Calcium recordings were made during the following sessions, late (stable) self-

72 administration (two separate recordings across days 8-12), during the first day post-abstinence

73 (PA) and during the final cue-only reinstatement session (Figure 1d). D1- and D2-Cre mice showed

74 equivalent levels of self-administration across reward and genotype modalities (Figures 1e,f).

75 Similarly, equivalent rewarded active nose-poking between D1- and D2-Cre mice was observed

76 during the PA session and extinction training (Figures 1g,h and S1a,c). However, akin to previous

77 findings[4,15], D1- and D2-Cre mice reinstated more to cocaine cues than sucrose cues (Figure 1i).

78 Inactive NPs were not different between D1- and D2-Cre mice in rewarded (Figure 1e,f) or

79 unrewarded (Figure S1) seeking. No sex differences appeared in any of the behavioral measures

80 shown in Figure 1 (Figure S2).

81 *Total Ca^{2+} activity per neuron:*

82 We first quantified the total number of excitatory Ca^{2+} events for each D1- or D2-MSN. While no

83 difference between sucrose and cocaine was found during self-administration (Figure S3a),

84 cocaine PA seeking produced more Ca^{2+} events in D1-MSNs than sucrose, with equivalent event

85 number between rewards in D2-MSNs (Figure S3b). For cued reinstatement the number of Ca^{2+}

86 events in cocaine exceeded sucrose mice for both D1- and D2-MSNs (Figure S3c). Together these

87 data indicate that for unrewarded seeking cocaine-trained mice showed more Ca^{2+} activity,

88 especially in D1-MSNs where cocaine exceeded sucrose in both PA and reinstatement sessions

89 (Figure S3d). In contrast, when a reward was delivered during self-administration the activity of

90 both D1- and D2-MSNs was equivalent between cocaine and sucrose.

91 *Time-locked population mean of NP-induced Ca^{2+} activity:*

92 Rewarded seeking. We next time-locked Ca^{2+} activity in D1- or D2-MSNs to reinforced active

93 NPs during self-administration. Heatmaps of averaged activity of D1- and D2-MSN indicated

94 similar heterogenous response of neurons regardless of MSN subtype or reward, with some

95 neurons activated and others inhibited around rewarded NPs (Figure 2a). Considering the

96 heterogeneity of responses, we first averaged and compared the time-locked activity of neurons

97 around rewarded NPs in sucrose and cocaine trained animals. Mean population activity was

98 compared to a null distribution generated by randomly shuffling the data around the NP

99 timestamps 1000x (95% CI was used for statistical significance). Population-averaged D1-MSN

100 activity showed an early (0-2 sec after NP) and late (4-6 sec) excitation associated with cocaine

101 self-administration, compared to an early excitation and late inhibition associated with sucrose

102 self-administration (5-10 sec; Figure 2b). The comparable early excitation likely resulted from

103 nose-poking for either reward, while the late differences between sucrose and cocaine delivery

6

104   may be explained by differences in the reward delivered. Sucrose pellets were dispensed from a

105   second port after the NP activated cue consumption, allowing us to accurately time-lock activity

106   around NPs at the sucrose delivery port, directly associated with reward retrieval. The late decrease

107   in D1-MSN activity corresponded to accessing sucrose pellet in the 2nd port (Figure S4). Although

108   not directly measured here, it is estimated that intravenous cocaine accesses the rodent brain within

109   3-7 sec[16], supporting the possibility that the late D1-MSN excitatory response corresponded to

110   cocaine delivery, especially considering that cocaine-induced increases in extracellular dopamine

111   would promote depolarization of D1-MSNs[17]. Differences between sucrose and cocaine were also

112   measured in D2-MSNs showing early excitation for cocaine and no significant change for sucrose

113   (Figure 2c). D2-MSNs in cocaine administering mice also showed late (4-7 sec) reduction in

114   activity, possibly a pharmacological effect of cocaine since a cocaine-induced rise in extracellular

115   dopamine would be expected to promote hyperpolarization of D2-MSNs[17].

116   Unrewarded seeking. D1- and D2-MSN individual activity contained heterogenous responses to

117   NPs for unrewarded sucrose- and cocaine-seeking (Figure 2c,e). Population mean activity of all

118   recorded neurons revealed differences between sucrose and cocaine PA (Figure 2d) and cue-

119   reinstated seeking (Figure 2f). Population-averaged D1-MSN activity around NPs for cocaine PA

120   rapidly increased (peak=+1 sec), while a slightly delayed decrease was observed for sucrose

121   seeking (peak=+2 sec). Moreover, D1-MSN activity was inhibited in cocaine mice between 4-9

122   sec after the NP. D2-MSN activity was increased by PA seeking for both rewards peaking

123   immediately after NP and gradually returning to baseline.

124   The average time-locked cue reinstated response across all neurons differed for D1-MSNs between

125   sucrose and cocaine (Figure 2e). Cocaine cue-reinstated NPs were associated with a rapid increase

126   in time-locked activity while no averaged time-locked activity was recorded in sucrose mice

7

127   (Figure 2f). Neither sucrose nor cocaine time-locked NPs during cued reinstatement were

128   associated with a change in overall activity in D2-MSNs (Figure 2f).

129   Taken together, the most striking feature in these data was that rewarded and unrewarded cocaine

130   seeking activity was associated with consistent excitatory responses in D1-MSNs (Figure 2g). In

131   contrast, D1-MSN responses to sucrose seeking activity varied depending on the session and

132   reward availability, from increase to decrease to no change.

133   ***Subpopulations of MSNs time-locked to NPs:***

134   Rewarded Seeking. Due to the heterogeneity of the neuronal responses recorded around seeking

135   NPs, we clustered individual neurons into subpopulations based on their time-locked peri-NP

136   activity over the 5 sec before and 10 sec after rewarded NPs. Individual neurons were parsed into

137   excited, inhibited or not time-locked, by comparing their mean activity across all trials to a null

138   distribution generated by shuffling the Ca^{2+} activity around behavioral responses (1000x iterations,

139   95% confidence interval; Figure 3a,b and Figures S5-6; see Methods for details). The

140   subpopulations of neurons were compared between cocaine- and sucrose-trained mice across the

141   behavioral protocol in Figure 1d, including during self-administration, PA seeking, and cued

142   reinstatement.

143   During rewarded self-administration, sucrose NPs yielded a higher proportion of time-locked

144   excited and inhibited subpopulations of D1- and D2-MSNs than cocaine NPs (Figure 3c). Notably,

145   the activity of excited D1-MSNs during cocaine self-administration showed a bimodal distribution

146   (figure S5), akin to that of the mean population activity (Figure 2c). The bimodal distribution is

147   consistent with two different populations of excited D1-MSNs, the first activated between 0-

148   2seconds, and the second activated between 3-7 seconds, which supports the earlier conclusion

8

149   that the two peaks may be due to an early cue response, followed by a delayed pharmacological

150   cocaine-mediated excitatory response.

151   Unrewarded Seeking: During PA seeking, the proportion of subpopulations of D1- and D2-MSNs

152   showing excitation, inhibition, both or not time-locked were comparable in size between sucrose-

153   and cocaine-trained mice (Figure 3d). Notably, cue reinstated cocaine seeking recruited more

154   overall time-locked D1-MSNs than sucrose seeking, which was explained predominantly by a

155   nearly 2-fold increase in excited D1-MSNs (Figure 3e,f). In general, time-locked excited D1-

156   MSNs were more excited and more synchronized around NPs during unrewarded cocaine seeking

157   sessions compared to sucrose (Figure S5), while time-locked inhibited neurons were more

158   inhibited during sucrose seeking sessions compared to cocaine (Figure S6). On the other hand, the

159   proportions of D2-MSN showed no differences between sucrose or cocaine during unrewarded

160   post-abstinence or reinstated seeking during (Figure 3d,e).

161   Taken together (Figure 3f), these data indicate that during self-administration, when the reward is

162   available, sucrose reinforcement is recruiting more excited and inhibited D1- and D2-MSNs,

163   perhaps contributing to the fact that when given a choice, rodents prefer food over cocaine

164   reward[4,15] (however, see[18]). When the reward is omitted during cued reinstatement test, cocaine

165   associated NPs and cues recruit more excited and inhibited D1-MSNs than sucrose associated

166   NP/cues.

167   ***Stability of time-locked activity within a seeking session:***

168   We tracked time-locked individual neurons across the course of a seeking session to determine if

169   the responses of neuronal subpopulations were stable or different neurons were recruited to the

170   time-locked excited and inhibited subpopulations of MSNs. Stability was estimated by time-

171   locking to odd- or even-numbered NPs, and if an MSN was time-locked to both sets of events, it

172   was considered stable (Figure 4a shows examples of stable and unstable neurons).

173   <u>Stability of time-locked activity during reward seeking.</u> For either self-administered rewards, the

174   proportion of stable excited D1-MSNs trended (p= 0.059) higher in cocaine than sucrose self-

175   administration. No other differences in stability were evident between sucrose and cocaine across

176   the subpopulations.

177   <u>Stability of time-locked activity during unrewarded seeking.</u> We performed the same

178   subpopulation stability analyses for both the PA seeking and cue reinstatement. During the PA

179   session the odd/even analysis for stability showed two major differences (Figure 4c). Excited D1-

180   MSNs in cocaine mice were more stable than sucrose excited D1-MSNs. Also, inhibited D2-MSNs

181   in cocaine mice were remarkably unstable and showed less stability than sucrose inhibited D2-

182   MSNs.

183   The odd/even analysis for cued reinstatement showed that excited D1-MSNs trended (p= 0.068)

184   towards being more stable in cocaine compared to sucrose mice (Figure 4d). No other differences

185   in stability between sucrose and cocaine were evident between sucrose and cocaine across the

186   subpopulations.

187   The patterns of subgroup stability across the three different seeking sessions are summarized in

188   Figure 4e, which illustrates the percent difference in stable MSNs between cocaine and sucrose.

189   The primary result is that excited D1-MSNs are more stable in response to active seeking in

190   cocaine- compared with sucrose-trained mice, regardless of the type of seeking session (self-

191   administration, PA or cued reinstatement). Also, relative to sucrose, cocaine mice had fewer stable

192   inhibited D2-MSNs in the PA session.

10

193   Correlations between time-locked subpopulations and NPs.   We examined if the neuronal

194   subpopulations were statistically associated with cued active NPs by linear regression comparisons

195   between cued NPs and the percent of neurons in each subgroup. Combining D1- and D2-MSNs

196   revealed that cocaine excited MSNs were correlated with NPs during self-administration and PA

197   seeking and cocaine inhibited MSNs correlated with NPs during self-administration (Table S2).

198   When the MSNs were separated into the excited D1- and D2-MSN subpopulations, only cocaine

199   excited D1-MSNs remained correlated with NPs during self-administration and PA (Figure 4f,

200   Table S2). Similarly, only inhibited D1-MSNs were correlated with cocaine NPs (Figure 4f). No

201   correlations were observed during cued-reinstatement, nor in sucrose seeking for any

202   subpopulation of MSNs (Figure 4f; Table S2).

203   ***Decoding NP initiation using MSN subpopulations:***

204   Neuronal responses preceding NPs may represent a motivational signal to seek the reward. We

205   used machine learning (Figure S7) to determine if Ca^{2+} data from time-locked subpopulations of

206   D1- and D2-MSNs could decode the initiation of an NP (activity during the 5 sec preceding NP).

207   The decoding accuracy in shuffled datasets of random events were used as control and were

208   subtracted from the quantified time-locked data in each subgroup for each animal in the study.

209   Rewarded NPs during self-administration were decoded by excited D1-MSNs in sucrose and

210   cocaine mice and excited D2-MSNs only in cocaine mice (Figure 5). Only in cocaine mice did

211   inhibited D1-MSNS effectively decode NPs. Surprisingly, MSNs that were not time-locked

212   decoded sucrose, but not cocaine rewarded NPs for both D1- and D2-MSNs. Akin to rewarded

213   NPs, for both sucrose and cocaine PA seeking excited D1-MSNs predicted NPs and inhibited D1-

214   MSNs decoded only cocaine NPs (Figure 5a). Excited D2-MSNs also predicted PA NPs for

215   cocaine, but not sucrose (Figure 5b). During cued reinstatement excited D1-MSNs decoded NPs

216   only in cocaine mice and no other subgroup of D1- or D2-MSNs successfully decoded sucrose or

217   cocaine NPs. Figure 5c summarizes the capacity of subpopulations of MSNs to decode cocaine

218   and sucrose NPs in all three behavioral sessions. Similar to the above observations of

219   subpopulation stability and overall activity (Figures 3f, 4e), only excited D1-MSNs decoded NPs

220   in all three cocaine seeking sessions. Also, it was surprising that for sucrose rewarded NPs both

221   the D1- and D2-MSNs that were not time-locked predicted the NPs. This argues that other

222   subpopulations not identified using our time-locking algorithm may be contributing to sucrose but

223   not cocaine self-administration.

224   ***Stability of time-locked activity between self-administration sessions.***

225   Lastly, we determined if time-locked subpopulations of MSNs were stable longitudinally between

226   different rewarded self-administration sessions, and if the same neurons associated with cocaine

227   self-administration had similar responding in a subsequent unrewarded PA session. Neurons

228   between multiple sessions were tracked using a previously established nearest-neighbor cell

229   registration method[19] (Figure 6a). The same D1-MSN and D2-MSN were tracked between two

230   late sucrose and cocaine self-administration sessions (Figure 6b,c) where mouse self-

231   administration was stable and reliable (day 7-9 versus 10-12, respectively). Neurons were termed

232   stable if they showed similar time-locked responses during the first and second self-administration

233   sessions. There was no difference in stability between sucrose and cocaine rewarded seeking in

234   either of the D1- or D2-MSN subpopulations (Figure 6b,c; Table S4 for statistical values). To

235   verify if neuronal responses are preserved across multiple self-administration sessions, we used

236   machine learning to train an SVM model on tracked neurons from an early self-administration

237   session (day 7-9) to decode NPs from a later self-administration session (days 10-12). Tracked D1-

238   MSNs, but not D2-MSNs, from one self-administration session successfully decoded seeking

239 behavior from the other session in cocaine and sucrose trained animals (Figure 6d; Table S5 for

240 statistical values). This indicates that a relatively stable neuronal representation of D1-MSNs was

241 formed during self-administration in both reward subtypes.

Stability of time-locked activity between rewarded and unrewarded sessions.

243 One key aspect of drug seeking behavior is the long-lasting associations made between drug

244 seeking and drug-associated cues, whereby associated cues gain salience to drive behavior despite

245 an extended period of abstinence. We asked if the neuronal representations that we recorded during

246 cocaine and sucrose self-administration were carried forward into unrewarded PA seeking

247 sessions, with the overarching hypothesis that stable neuronal representations are likely

248 responsible for the prepotent seeking for cocaine over sucrose. We longitudinally tracked neurons

249 between the last self-administration session (day 10-12) into the PA session conducted after 7-10

250 days of abstinence. Akin to the within session stability measurements (Figure 4), excited cocaine

251 D1-MSNs were more stable than sucrose D1-MSNs across the two sessions (Figure 6e; Table S4).

252 We also trained machine learning models on the recorded data from tracked neurons from self-

253 administration session to decode NPs during PA sessions. Interestingly, only cocaine D1-MSNs

254 that tracked from self-administration to PA sessions accurately decoded seeking in the PA session

255 (Figure 6g; Table S5 for statistical values), indicating a stable and persistent representation of

256 cocaine seeking compared to sucrose seeking despite an extended period of abstinence.

257 Together with the within session stability data (Figure 4) and the overall responsiveness time-

258 locked D1- and D2-MSNs (Figure 2), the across-session stability further emphasizes the role of

259 greater excited D1-MSN stability in cocaine versus sucrose trained mice across the rewarded and

260 unrewarded (PA) seeking modalities, indicative of a stable long-term ensemble consistently

261 recruited during cocaine seeking events.

13

DISCUSSION

We used a variety of analytical approaches to determine if cocaine and sucrose seeking involved neuronal activity in distinct subpopulations NAcore MSNs, with the overarching hypothesis that any differences discovered might contribute to why individuals with cocaine use disorder are more motivated by cues predicting cocaine over natural rewards. Using single cell Ca^{2+} imaging as a measure of neuronal activity allowed us to quantify activity in specific subpopulations of D1- and D2- MSNs and to longitudinally track the subpopulations within and between rewarded and unrewarded seeking[19]. The most striking and consistent distinction we discovered between sucrose and cocaine seeking was that excited D1-MSNs show greater overall activity, stability and capacity to decode cocaine seeking behavior compared to sucrose seeking. This difference in D1-MSN activity between cocaine and sucrose seeking was most evident during unrewarded cocaine seeking (PA and cue reinstated seeking). In contrast, similar patterns of activity in D1- and D2-MSNs were often manifested by sucrose and cocaine seeking when the reward was available during self-administration.

During rewarded self-administration sessions, both reward types were associated with comparable peri-NP excitation of D1-MSNs, similar heterogeneity of responses across excited/inhibited subpopulations, and comparable decoding accuracy of D1- and D2- neuronal data to predict NPs. However, a difference between sucrose and cocaine in D1-MSN activity was observed between 5-10 sec after the rewarded NP that likely corresponded to receipt of the reward. Cocaine showed an delayed excitatory response associated with intravenous cocaine delivery that contrasted with a delayed inhibitory response associated with sucrose reward consumption. Interestingly, distinct and non-overlapping subpopulations of excited D1-MSNs were associated with the immediate NP and the subsequent delayed response to reward, suggesting different neuronal ensembles and

14

285   possibly brain circuits involved in each response[11]. While the cocaine-associated delayed increase

286   is consistent with cocaine's increase in dopamine stimulation of D1-dopamine receptors[20], the

287   findings that sucrose retrieval was associated with a decrease rather than an increase in D1-MSNs

288   activity of the NAcore was surprising but consistent with previous in vivo electrophysiological

289   recordings from the nucleus accumbens during food consumption[21,22].

290   While excited D1-MSNs were also associated with rewarded sucrose seeking by some measures,

291   the activity was not as consistent as with cocaine for unrewarded seeking. For example, excited

292   D1-MSN activity during unrewarded cocaine sessions was notably more robust, of higher

293   amplitude and more synchronized around seeking activity (Figure S5). Also, our different

294   measures of neuronal stability showed a higher consistency within the excited D1-MSN

295   subpopulation in cocaine-trained animals compared to sucrose in unrewarded sessions.

296   Furthermore, excited D1-MSNs decoded and predicted NPs only in cocaine, not sucrose cue

297   seeking. Together, these findings indicate that an excited D1-MSN subpopulation formed a

298   consistent and stable ensemble mobilized by unrewarded cocaine seeking. Importantly, while this

299   ensemble was formed and stable for both sucrose and cocaine self-administration, only the cocaine

300   excited D1-MSN ensemble persisted into unrewarded PA seeking. In contrast, the parallel

301   ensemble of excited D1-MSNs present during sucrose self-administration did not reform during

302   PA seeking for sucrose. In conclusion, an excited D1-MSN ensemble formed during self-

303   administration of either cocaine or sucrose, but propagated to unrewarded seeking only in cocaine-

304   trained mice. This conclusion is buttressed by finding that only excited D1-MSN activity

305   correlated with the intensity of cocaine PA seeking, while no subpopulation of MSNs correlated

306   with sucrose behavioral seeking. Moreover, we replicated our previous findings and the findings

307   of others[4,15], that cue reinstated seeking is greater for cocaine than sucrose cues.

308   The partial similarity between the excited D1-MSN subpopulations during rewarded cocaine or

309   sucrose seeking and the striking difference in this subpopulation during unrewarded sucrose versus

310   cocaine seeking, raises an important question. What mediates the propagation of the excited D1-

311   MSN subpopulation from rewarded into unrewarded seeking only in cocaine mice? Indicative of

312   potentiated D1-MSNs synapses, non-contingent or self-administered cocaine infusions produce

313   enduring increases in dendritic spine density and spine head diameter selectively in accumbens

314   D1-MSNs[23-25]. This is paralleled by an increase in AMPA glutamate receptor mediated currents

315   after extended withdrawal from cocaine self-administration[26-28]. Importantly, enduring

316   potentiation is found selectively in D1-MSNs after abstinence from cocaine, not sucrose self-

317   administration[29]. While the enduring adaptations induced by cocaine, not sucrose, demonstrate a

318   mechanism whereby D1-MSN excitatory responses to glutamate release are potentiated for weeks

319   after discontinuing drug use, measurements of synaptic potentiation during unrewarded seeking

320   reveal that cocaine, but not sucrose cues elicit further potentiation that is transiently expressed only

321   for the duration of a seeking session[30]. For example, ex vivo measures of synaptic potentiation,

322   including increased AMPA/NMDA ratio and dendritic spine head diameter, are transiently

323   elevated only in D1-MSNs during cued cocaine, not sucrose seeking[29,31]. This is paralleled by

324   increased extracellular matrix signaling through b3-integrins selectively in D1-MSNs[32-34] and

325   decreased astroglial synaptic proximity during cued seeking for cocaine or heroin, not sucrose[35].

326   Combined these data are highly consistent with our Ca^{2+} activity measurements revealing an

327   ensemble of excited D1-MSNs associated with NPs for cocaine PA and cued reinstatement, but

328   not for unrewarded sucrose seeking. Furthermore, the data offer a mechanism by which this occurs,

329   via both enduring synaptic potentiation in withdrawal and transient synaptic potentiation that

16

330   depends on temporary adaptations in astroglial morphology and signaling in the extracellular

331   matrix.

332   A role for D1-MSNs as key regulators of reward seeking is consistent with a variety of

333   optogenetic[36] and DREADD stimulation and inhibition[31,37,38] studies concluding that activity in

334   D1-MSNs is sufficient and necessary for rewarded and unrewarded cue seeking[4,30,31]. Conversely,

335   these studies generally conclude that activity in D2-MSNs serves an opposing function to reduce

336   reward seeking[30,31,37,39]. However, optogenetic and DREADD studies indiscriminately stimulate

337   or inhibit D1- or D2-MSNs, which does not reflect the electrophysiological and imaging

338   observations that subpopulations of MSNs can be active and inhibited during a seeking event

339   regardless of genotype[5,7]. In accord with the importance of this caveat, the functional dichotomy

340   between D1- and D2-MSNs is being challenged by studies showing a more nuanced collaborative

341   role between MSN subpopulations[40-42]. For example, if animals undergoing operant food seeking

342   are tested during periods of reward unavailability, fiber photometry recordings reveal increased

343   Ca^{2+} activity in both MSN subtypes, and inhibiting either subtype results in associated increases

344   of unproductive reward seeking[43]. Also, 2-photon imaging from the shell subcompartment of

345   nucleus accumbens shows that distinct functional clusters of both D1- and D2-MSNs encode the

346   intensity of sucrose rewards versus consummatory (i.e. licking) behavior[44]. Furthermore, a recent

347   examination of how valence of a conditioned stimulus controls operant responding concluded that

348   D1- and D2-MSNs collaborate to provide information regarding specific valence-independent

349   associative learning[45] . Finally, the dichotomous model of D1- and D2-MSN functioning fails to

350   account for further genetic heterogeneity within each subtype, such as a recently identified

351   subpopulation of D1-MSNs expressing tachykinin-2 that negatively regulates cocaine seeking

352   behavior[46]. While our study reveals both excited and inhibited subpopulations of D1- and D2-

353   MSNs in the NAcore can be associated with both cocaine and sucrose seeking, only the excited

354   D1-MSN population was stable and predictive of unrewarded cocaine, not sucrose seeking.

355   Nonetheless, these data do not discount a role for other subpopulations of MSNs contributing to

356   both cocaine and sucrose seeking. Consistent with this idea, there is ~25% overlap between

357   neurons labeled for the IEG c-fos during cue-induced cocaine and sucrose seeking[4].

358   Our experiments show that cocaine seeking is associated with a stable ensemble of D1-MSNs

359   activity within rewarded seeking sessions that persists for at least 10 days of abstinence into a post-

360   abstinence seeking session. Stability of individual neuronal activity within the 120 min rewarded

361   and unrewarded seeking sessions as well as longitudinally after 10 days of abstinence between a

362   rewarded and unrewarded sessions strongly argues that a discrete ensemble of excited D1-MSNs

363   is formed during self-administration and becomes critical for unrewarded cocaine seeking.

364   Conversely, the relative instability and poor decoding of time-locked MSN responses during

365   unrewarded sucrose seeking is consistent with network level neuronal encoding that likely

366   involves recruitment of shifting populations of D1- and D2-MSNs to guide behavior. This

367   interpretation resonates with behavioral studies directly comparing cocaine and sucrose seeking

368   that generally show neuronal activity in the NAcore is obligatory for cued reinstatement of cocaine,

369   but not sucrose seeking[31,47,48]. Thus, sucrose seeking involves a more distributed network in the

370   brain that can function in the absence of NAcore neurons, possibly reflecting the survival necessity

371   of food seeking[10]. In contrast, cocaine seeking is associated with drug-induced enduring and

372   transient neuroadaptations selective for NAcore D1-MSNs that favor the formation of an excited

373   D1-MSN ensemble underpinning cocaine NPs[29,30,49]. Based on our observations of a cocaine, not

374   sucrose seeking ensemble of excited D1-MSNs and other findings identifying long-lasting and

375   cue-induced transient adaptations by cocaine over sucrose seeking, we hypothesize it is the

376   formation of this ensemble that causes cocaine cues to more potently drive seeking compared to

377   sucrose cues[4,50,51], and contributes to why individuals suffering cocaine use disorder seek cocaine

378   in response to cocaine-associated stimuli in preference to seeking natural rewards.

ACKNOWLEDGMENTS

382   Author Contributions: Conceptualization, R.M.C. and P.W.K.; Methodology, R.M.C. and P.W.K.;

383   Investigation, R.M.C., A.T., J.H., and C.C.; Software and Data Curation: R.M.C. Writing –

384   Original Draft, R.M.C. and P.W.K.; Writing – Review & Editing, R.M.C. and P.W.K.; Funding

385   Acquisition, R.M.C. and P.W.K.; Visualization: R.M.C. and P.W.K.

386   Declaration of Interests: the authors declare no competing interests.

SUPPLEMENTAL INFORMATION:

388   Document S1. Supplemental figures (S1-S6)

389   Document S2. Supplemental tables (T1-T5)

390 REFERENCES:

391 1. Pennartz, C.M.A., Groenewegen, H.J., and Lopes da Silva, F.H. (1994). The nucleus accumbens as
392 a complex of functionally distinct neuronal ensembles: An integration of behavioural,
393 electrophysiological and anatomical data. Progress in Neurobiology *42*, 719-761.
394 https://doi.org/10.1016/0301-0082(94)90025-6.
395 2. Bobadilla, A.-C., Heinsbroek, J.A., Gipson, C.D., Griffin, W.C., Fowler, C.D., Kenny, P.J., and
396 Kalivas, P.W. (2017). Chapter 4 - Corticostriatal plasticity, neuronal ensembles, and regulation of
397 drug-seeking behavior. In Progress in Brain Research, T. Calvey, and W.M.U. Daniels, eds.
398 (Elsevier), pp. 93-112. https://doi.org/10.1016/bs.pbr.2017.07.013.
399 3. Cruz, F.C., Koya, E., Guez-Barber, D.H., Bossert, J.M., Lupica, C.R., Shaham, Y., and Hope, B.T.
400 (2013). New technologies for examining the role of neuronal ensembles in drug addiction and
401 fear. Nature Reviews Neuroscience *14*, 743-754. 10.1038/nrn3597.
402 4. Bobadilla, A.-C., Dereschewitz, E., Vaccaro, L., Heinsbroek, J.A., Scofield, M.D., and Kalivas, P.W.
403 (2020). Cocaine and sucrose rewards recruit different seeking ensembles in the nucleus
404 accumbens core. Molecular Psychiatry *25*, 3150-3163. 10.1038/s41380-020-00888-z.
405 5. Carelli, R.M. (2002). Nucleus accumbens cell firing during goal-directed behaviors for cocaine vs.
406 'natural' reinforcement. Physiology & behavior *76*, 379-387. https://doi.org/10.1016/S0031-
407 9384(02)00760-6.
408 6. Roitman, M.F., Wheeler, R.A., and Carelli, R.M. (2005). Nucleus accumbens neurons are innately
409 tuned for rewarding and aversive taste stimuli, encode their predictors, and are linked to motor
410 output. Neuron *45*, 587-597. 10.1016/j.neuron.2004.12.055.
411 7. Van Zessen, R., Li, Y., Marion-Poll, L., Hulo, N., Flakowski, J., and Lüscher, C. (2021). Dynamic
412 dichotomy of accumbal population activity underlies cocaine sensitization. eLife *10*.
413 10.7554/elife.66048.
414 8. Grant, R.I., Doncheck, E.M., Vollmer, K.M., Winston, K.T., Romanova, E.V., Siegler, P.N., Holman,
415 H., Bowen, C.W., and Otis, J.M. (2021). Specialized coding patterns among dorsomedial
416 prefrontal neuronal ensembles predict conditioned reward seeking. eLife *10*.
417 10.7554/elife.65764.
418 9. Taniguchi, M., Carreira, M.B., Cooper, Y.A., Bobadilla, A.C., Heinsbroek, J.A., Koike, N., Larson,
419 E.B., Balmuth, E.A., Hughes, B.W., Penrod, R.D., et al. (2017). HDAC5 and Its Target Gene, Npas4,
420 Function in the Nucleus Accumbens to Regulate Cocaine-Conditioned Behaviors. Neuron *96*,
421 130-144.e136. 10.1016/j.neuron.2017.09.015.
422 10. Sortman, B.W., Rakela, S., Paprotna, S., Cerci, B., and Warren, B.L. (2024). Nucleus accumbens
423 neuronal ensembles vary with cocaine reinforcement in male and female rats. Addict Biol *29*,
424 e13397. 10.1111/adb.13397.
425 11. Scofield, M.D., Heinsbroek, J.A., Gipson, C.D., Kupchik, Y.M., Spencer, S., Smith, A.C.W., Roberts-
426 Wolfe, D., and Kalivas, P.W. (2016). The Nucleus Accumbens: Mechanisms of Addiction across
427 Drug Classes Reflect the Importance of Glutamate Homeostasis. Pharmacological Reviews *68*,
428 816-871. 10.1124/pr.116.012484.
429 12. Carelli, R.M., and Wondolowski, J. (2003). Selective Encoding of Cocaine versus Natural Rewards
430 by Nucleus Accumbens Neurons Is Not Related to Chronic Drug Exposure. The Journal of
431 Neuroscience *23*, 11214-11223. 10.1523/jneurosci.23-35-11214.2003.
432 13. Namboodiri, V.M.K., Otis, J.M., van Heeswijk, K., Voets, E.S., Alghorazi, R.A., Rodriguez-
433 Romaguera, J., Mihalas, S., and Stuber, G.D. (2019). Single-cell activity tracking reveals that
434 orbitofrontal neurons acquire and maintain a long-term memory to guide behavioral adaptation.
435 Nature Neuroscience *22*, 1110-1121. 10.1038/s41593-019-0408-1.

20

436 14. Resendez, S.L., Jennings, J.H., Ung, R.L., Namboodiri, V.M.K., Zhou, Z.C., Otis, J.M., Nomura, H.,
437   McHenry, J.A., Kosyk, O., and Stuber, G.D. (2016). Visualization of cortical, subcortical and deep
438   brain neural circuit dynamics during naturalistic mammalian behavior with head-mounted
439   microscopes and chronically implanted lenses. Nature Protocols *11*, 566.
440   10.1038/nprot.2016.021.
441 15. Tunstall, B.J., and Kearns, D.N. (2016). Cocaine can generate a stronger conditioned reinforcer
442   than food despite being a weaker primary reinforcer. Addict Biol *21*, 282-293.
443   10.1111/adb.12195.
444 16. Wise, R.A., and Kiyatkin, E.A. (2011). Differentiating the rapid actions of cocaine. Nature Reviews
445   Neuroscience *12*, 479-484. 10.1038/nrn3043.
446 17. Surmeier, D.J., Ding, J., Day, M., Wang, Z., and Shen, W. (2007). D1 and D2 dopamine-receptor
447   modulation of striatal glutamatergic signaling in striatal medium spiny neurons. Trends in
448   neurosciences *30*, 228-235. S0166-2236(07)00069-0 [pii]

449 10.1016/j.tins.2007.03.008.
450 18. Canchy, L., Girardeau, P., Durand, A., Vouillac-Mendoza, C., and Ahmed, S.H. (2021).
451   Pharmacokinetics trumps pharmacodynamics during cocaine choice: a reconciliation with the
452   dopamine hypothesis of addiction. Neuropsychopharmacology *46*, 288-296. 10.1038/s41386-
453   020-0786-9.
454 19. Sheintuch, L., Rubin, A., Brande-Eilat, N., Geva, N., Sadeh, N., Pinchasof, O., and Ziv, Y. (2017).
455   Tracking the Same Neurons across Multiple Days in Ca2+ Imaging Data. Cell Reports *21*, 1102-
456   1115. https://doi.org/10.1016/j.celrep.2017.10.013.
457 20. Stuber, G.D., Roitman, M.F., Phillips, P.E.M., Carelli, R.M., and Wightman, R.M. (2005). Rapid
458   Dopamine Signaling in the Nucleus Accumbens during Contingent and Noncontingent Cocaine
459   Administration. Neuropsychopharmacology *30*, 853-863. 10.1038/sj.npp.1300619.
460 21. Lee, R.S., Koob, G.F., and Henriksen, S.J. (1998). Electrophysiological responses of nucleus
461   accumbens neurons to novelty stimuli and exploratory behavior in the awake, unrestrained rat.
462   Brain Res *799*, 317-322. 10.1016/s0006-8993(98)00477-6.
463 22. Eoin, Kremer, Y., Lefort, S., Harada, M., Pascoli, V., Rohner, C., and Lüscher, C. (2015). Accumbal
464   D1R Neurons Projecting to Lateral Hypothalamus Authorize Feeding. Neuron *88*, 553-564.
465   10.1016/j.neuron.2015.09.038.
466 23. Smith, R.J., Lobo, M.K., Spencer, S., and Kalivas, P.W. (2013). Cocaine-induced adaptations in D1
467   and D2 accumbens projection neurons (a dichotomy not necessarily synonymous with direct and
468   indirect pathways). Curr Opin Neurobiol *23*, 546-552. 10.1016/j.conb.2013.01.026.
469 24. Anderson, E.M., and Self, D.W. (2017). It's only a matter of time: longevity of cocaine-induced
470   changes in dendritic spine density in the nucleus accumbens. Curr Opin Behav Sci *13*, 117-123.
471   10.1016/j.cobeha.2016.11.013.
472 25. Kim, J., Park, B.H., Lee, J.H., Park, S.K., and Kim, J.H. (2011). Cell type-specific alterations in the
473   nucleus accumbens by repeated exposures to cocaine. Biological Psychiatry *69*, 1026-1034.
474   10.1016/j.biopsych.2011.01.013.
475 26. Ma, Y.Y., Lee, B.R., Wang, X., Guo, C., Liu, L., Cui, R., Lan, Y., Balcita-Pedicino, J.J., Wolf, M.E.,
476   Sesack, S.R., et al. (2014). Bidirectional modulation of incubation of cocaine craving by silent
477   synapse-based remodeling of prefrontal cortex to accumbens projections. Neuron *83*, 1453-
478   1467. 10.1016/j.neuron.2014.08.023.
479 27. Conrad, K.L., Tseng, K.Y., Uejima, J.L., Reimers, J.M., Heng, L.J., Shaham, Y., Marinelli, M., and
480   Wolf, M.E. (2008). Formation of accumbens GluR2-lacking AMPA receptors mediates incubation
481   of cocaine craving. Nature *454*, 118-121. 10.1038/nature06995.

28. Anderson, S.M., Famous, K.R., Sadri-Vakili, G., Kumaresan, V., Schmidt, H.D., Bass, C.E., Terwilliger, E.F., Cha, J.H., and Pierce, R.C. (2008). CaMKII: a biochemical bridge linking accumbens dopamine and glutamate systems in cocaine seeking. Nat Neurosci *11*, 344-353. https://doi.org/10.1038/nn2054.

29. Pascoli, V., Terrier, J., Espallergues, J., Valjent, E., O'Connor, E.C., and Lüscher, C. (2014). Contrasting forms of cocaine-evoked plasticity control components of relapse. Nature *509*, 459-464. 10.1038/nature13257.

30. Roberts-Wolfe, D., Bobadilla, A.-C., Heinsbroek, J.A., Neuhofer, D., and Kalivas, P.W. (2018). Drug Refraining and Seeking Potentiate Synapses on Distinct Populations of Accumbens Medium Spiny Neurons. The Journal of Neuroscience *38*, 7100-7107. 10.1523/jneurosci.0791-18.2018.

31. Heinsbroek, J.A., Neuhofer, D.N., Griffin, W.C., Siegel, G.S., Bobadilla, A.-C., Kupchik, Y.M., and Kalivas, P.W. (2017). Loss of Plasticity in the D2-Accumbens Pallidal Pathway Promotes Cocaine Seeking. The Journal of Neuroscience *37*, 757-767. 10.1523/jneurosci.2659-16.2016.

32. Garcia-Keller, C., Scofield, M.D., Neuhofer, D., Varanasi, S., Reeves, M.T., Hughes, B., Anderson, E., Richie, C.T., Mejias-Aponte, C., Pickel, J., et al. (2020). Relapse-Associated Transient Synaptic Potentiation Requires Integrin-Mediated Activation of Focal Adhesion Kinase and Cofilin in D1-Expressing Neurons. The Journal of neuroscience : the official journal of the Society for Neuroscience *40*, 8463-8477. 10.1523/JNEUROSCI.2666-19.2020.

33. Chioma, V.C., Kruyer, A., Bobadilla, A.C., Angelis, A., Ellison, Z., Hodebourg, R., Scofield, M.D., and Kalivas, P.W. (2021). Heroin Seeking and Extinction From Seeking Activate Matrix Metalloproteinases at Synapses on Distinct Subpopulations of Accumbens Cells. Biol Psychiatry *89*, 947-958. 10.1016/j.biopsych.2020.12.004.

34. Garcia-Keller, C., Neuhofer, D., Bobadilla, A.C., Spencer, S., Chioma, V.C., Monforton, C., and Kalivas, P.W. (2019). Extracellular Matrix Signaling Through beta3 Integrin Mediates Cocaine Cue-Induced Transient Synaptic Plasticity and Relapse. Biol Psychiatry *86*, 377-387. 10.1016/j.biopsych.2019.03.982.

35. Kruyer, A., and Kalivas, P.W. (2021). Astrocytes as cellular mediators of cue reactivity in addiction. Curr Opin Pharmacol *56*, 1-6. 10.1016/j.coph.2020.07.009.

36. Lobo, M.K., Covington, H.E., Chaudhury, D., Friedman, A.K., Sun, H., Damez-Werno, D., Dietz, D.M., Zaman, S., Koo, J.W., Kennedy, P.J., et al. (2010). Cell Type–Specific Loss of BDNF Signaling Mimics Optogenetic Control of Cocaine Reward. Science *330*, 385-390. 10.1126/science.1188472.

37. Pardo-Garcia, T.R., Garcia-Keller, C., Penaloza, T., Richie, C.T., Pickel, J., Hope, B.T., Harvey, B.K., Kalivas, P.W., and Heinsbroek, J.A. (2019). Ventral Pallidum Is the Primary Target for Accumbens D1 Projections Driving Cocaine Seeking. The Journal of Neuroscience *39*, 2041-2051. 10.1523/jneurosci.2822-18.2018.

38. Calipari, E.S., Bagot, R.C., Purushothaman, I., Davidson, T.J., Yorgason, J.T., Peña, C.J., Walker, D.M., Pirpinias, S.T., Guise, K.G., Ramakrishnan, C., et al. (2016). In vivo imaging identifies temporal signature of D1 and D2 medium spiny neurons in cocaine reward. Proceedings of the National Academy of Sciences *113*, 2726-2731. 10.1073/pnas.1521238113.

39. Bock, R., Shin, J.H., Kaplan, A.R., Dobi, A., Markey, E., Kramer, P.F., Gremel, C.M., Christensen, C.H., Adrover, M.F., and Alvarez, V.A. (2013). Strengthening the accumbal indirect pathway promotes resilience to compulsive cocaine use. Nat Neurosci *16*, 632-638. 10.1038/nn.3369.

40. Soares-Cunha, C., Coimbra, B., David-Pereira, A., Borges, S., Pinto, L., Costa, P., Sousa, N., and Rodrigues, A.J. (2016). Activation of D2 dopamine receptor-expressing neurons in the nucleus accumbens increases motivation. Nature Communications *7*, 11829. 10.1038/ncomms11829.

528 41. Soares-Cunha, C., Coimbra, B., Sousa, N., and Rodrigues, A.J. (2016). Reappraising striatal D1-
529   and D2-neurons in reward and aversion. Neuroscience & Biobehavioral Reviews *68*, 370-386.
530   10.1016/j.neubiorev.2016.05.021.
531 42. Soares-Cunha, C., Coimbra, B., Domingues, A.V., Vasconcelos, N., Sousa, N., and Rodrigues, A.J.
532   (2018). Nucleus Accumbens Microcircuit Underlying D2-MSN-Driven Increase in Motivation.
533   eNeuro *5*. 10.1523/eneuro.0386-18.2018.
534 43. Lafferty, C.K., Yang, A.K., Mendoza, J.A., and Britt, J.P. (2020). Nucleus Accumbens Cell Type- and
535   Input-Specific Suppression of Unproductive Reward Seeking. Cell Reports *30*, 3729-3742.e3723.
536   10.1016/j.celrep.2020.02.095.
537 44. Pedersen, C.E., Castro, D.C., Gray, M.M., Zhou, Z.C., Piantadosi, S.C., Gowrishankar, R., Kan, S.A.,
538   Murphy, P.J., O'Neill, P.R., and Bruchas, M.R. (2022). Medial accumbens shell spiny projection
539   neurons encode relative reward preference. Cold Spring Harbor Laboratory.
540 45. Zachry, J.E., Kutlu, M.G., Yoon, H.J., Leonard, M.Z., Chevée, M., Patel, D.D., Gaidici, A., Kondev,
541   V., Thibeault, K.C., Bethi, R., et al. (2024). D1 and D2 medium spiny neurons in the nucleus
542   accumbens core have distinct and valence-independent roles in learning. Neuron *112*, 835-
543   849.e837. 10.1016/j.neuron.2023.11.023.
544 46. Zhao, Z.D., Han, X., Chen, R., Liu, Y., Bhattacherjee, A., Chen, W., and Zhang, Y. (2022). A
545   molecularly defined D1 medium spiny neuron subtype negatively regulates cocaine addiction.
546   Sci Adv *8*, eabn3552. 10.1126/sciadv.abn3552.
547 47. McGlinchey, E.M., James, M.H., Mahler, S.V., Pantazis, C., and Aston-Jones, G. (2016). Prelimbic
548   to Accumbens Core Pathway Is Recruited in a Dopamine-Dependent Manner to Drive Cued
549   Reinstatement of Cocaine Seeking. The Journal of Neuroscience *36*, 8700-8711.
550   10.1523/jneurosci.1291-15.2016.
551 48. Nall, R.W., Heinsbroek, J.A., Nentwig, T.B., Kalivas, P.W., and Bobadilla, A.C. (2021). Circuit
552   selectivity in drug versus natural reward seeking behaviors. Journal of neurochemistry *157*,
553   1450-1472. 10.1111/jnc.15297.
554 49. Pascoli, V., Turiault, M., and Lüscher, C. (2012). Reversal of cocaine-evoked synaptic potentiation
555   resets drug-induced adaptive behaviour. Nature *481*, 71-75. 10.1038/nature10709.
556 50. Saunders, B.T., Yager, L.M., and Robinson, T.E. (2013). Cue-evoked cocaine "craving": role of
557   dopamine in the accumbens core. The Journal of neuroscience : the official journal of the
558   Society for Neuroscience *33*, 13989-14000. 10.1523/jneurosci.0450-13.2013.
559 51. Gipson, Cassandra D., Kupchik, Yonatan M., Shen, H., Reissner, Kathryn J., Thomas, Charles A.,
560   and Kalivas, Peter W. (2013). Relapse Induced by Cues Predicting Cocaine Depends on Rapid,
561   Transient Synaptic Potentiation. Neuron *77*, 867-872.
562   https://doi.org/10.1016/j.neuron.2013.01.005.
563 52. Heinsbroek, J.A., Bobadilla, A.C., Dereschewitz, E., Assali, A., Chalhoub, R.M., Cowan, C.W., and
564   Kalivas, P.W. (2020). Opposing Regulation of Cocaine Seeking by Glutamate and GABA Neurons
565   in the Ventral Pallidum. Cell Rep *30*, 2018-2027.e2013. 10.1016/j.celrep.2020.01.023.
566 53. Kmiotek, E.K., Baimel, C., and Gill, K.J. (2012). Methods for Intravenous Self Administration in a
567   Mouse Model. Journal of Visualized Experiments. 10.3791/3739.
568 54. Cameron, C.M., Murugan, M., Choi, J.Y., Engel, E.A., and Witten, I.B. (2019). Increased Cocaine
569   Motivation Is Associated with Degraded Spatial and Temporal Representations in IL-NAc
570   Neurons. Neuron *103*, 80-91.e87. 10.1016/j.neuron.2019.04.015.
571 55. Rubin, A., Geva, N., Sheintuch, L., and Ziv, Y. (2015). Hippocampal ensemble dynamics
572   timestamp events in long-term memory. eLife *4*, e12247. 10.7554/eLife.12247.

573

574

Figures and Legends
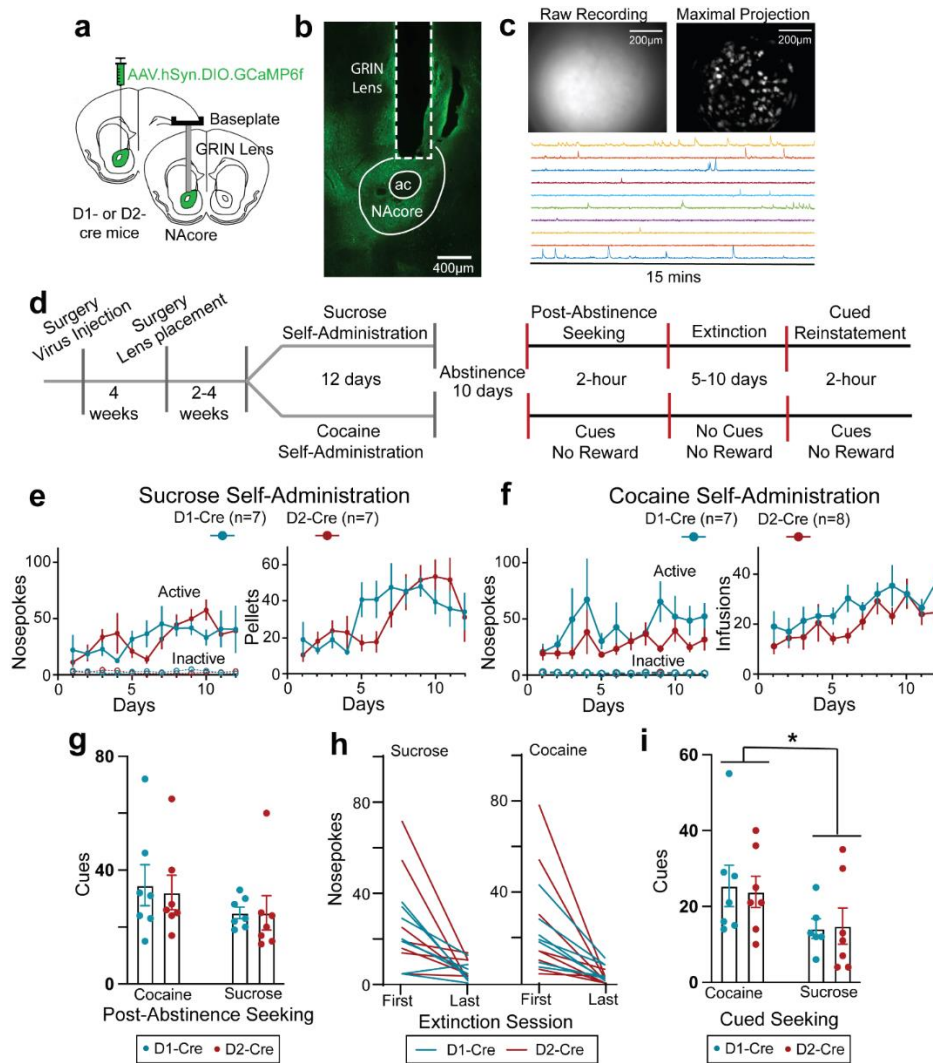
Figure 1. Single-cell resolution imaging of D1- and D2-MSN of nucleus accumbens core during sucrose/cocaine rewarded and unrewarded seeking.

(a) Illustration showing the surgical planning, including virus injection location and planned lens placement in D1- and D2-cre mice. (b) Micrograph from D1-cre mouse showing virus expression (stained with GFP+, green) and gradient index (GRIN) lens tract. (c) Field of view recording of a D1-cre mouse (upper left panel), the maximal intensity projection of the processed version (upper right panel), and example of temporal traces recorded from 10 random neurons (lower panel). (d) Schematic showing experimental design and timeline used to record Ca^{2+} activity from D1- and D2-MSNs during sucrose or cocaine self-

585   administration, post-abstinence seeking, and cued reinstatement. **(e)** D1-cre and D2-cre mice trained on

586   sucrose self-administration had similar total number of NPs per session (3-way ANOVA: Time x Genotype

587   x NP: $F_{(11,144)}$= 0.909, p=0.534; Genotype x NP: $F_{(1,144)}$= 0.056, p=0.814; Time x Genotype: $F_{(11,144)}$=

588   0.888, p=0.553; Time x NP: $F_{(11,144)}$= 1.973, p=0.035) and total number of sucrose pellets delivered per

589   session (Mixed Effects 2-way ANOVA: Time x Genotype: $F_{(11,149)}$= 1.724; p=0.073; Genotype: $F_{(1,14)}$=

590   1.125, p=0.307; Time: $F_{(4,56)}$= 7.201, p<0.001) over 12 days of sucrose self-administration. **(f)** D1 and D2-

591   cre mice trained on cocaine self-administration had similar total number of NPs per session (3-way

592   ANOVA: Time x Genotype x NP: $F_{(11,138)}$= 0.776, p=0.664; Genotype x NP: $F_{(1,138)}$= 1.978, p=0.162;

593   Time x Genotype: $F_{(11,138)}$= 0.701, p=0.736; Time x NP: $F_{(11,138)}$= 1.540, p=0.124; and total number of

594   cocaine infusions delivered per session (2-way ANOVA: Time x Genotype: $F_{(11,140)}$= 0.700, p=0.737;

595   Genotype: $F_{(1,13)}$= 3.113, p=0.101; Time: $F_{(11,140)}$= 3.938, p<0.001) over 12 days of cocaine self-

596   administration. **(g)** Number of rewarded NPs (cued) were comparable between sucrose- and cocaine-

597   trained D1- and D2-cre mice (2-way ANOVA: Cocaine Vs Sucrose: $F_{(1,24)}$= 2.198, p=0.151, Genotype:

598    $F_{(1,24)}$= 0.051, p=0.823, and interaction: $F_{(1,24)}$= 0.051, p=0.823). **(h)** Total number of NPs during first and

599   last extinction sessions in D1- and D2-cre mice trained on either cocaine (left) or sucrose (right). **(i)** Number

600   of rewarded NPs (cued) were higher in D1- and D2- cre mice trained on cocaine vs mice trained on sucrose

601   (2-way ANOVA: Cocaine Vs Sucrose: $F_{(1,23)}$= 5.100, p=0.0337, Genotype: $F_{(1,23)}$= 0.010, p=0.923, and

602   interaction: $F_{(1,23)}$= 0.064, p=0.803). *p<0.05

603

26
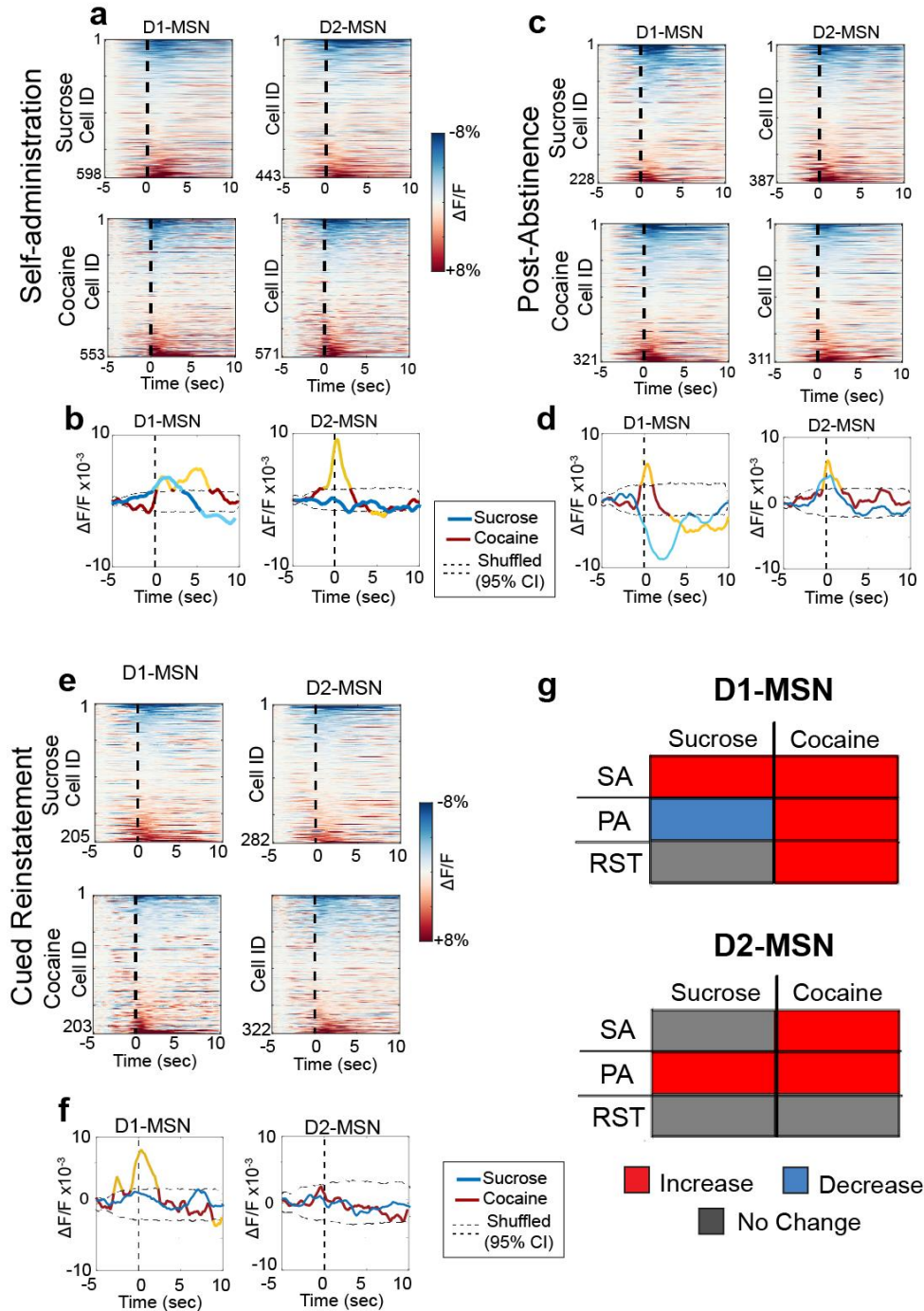
Figure 2. Different patterns of activity govern D1- and D2-MSN during rewarded and unrewarded cocaine/sucrose seeking. **(a)** Heatmaps representing the peristimulus histograms of the mean individual activity of recorded D1- (left) and D2-MSN (right) of mice previously trained on sucrose (upper) or cocaine (lower) around the first 10 cued active nosepoke during stable self-administration (SA7-12, 2 sessions per

609 animal), where active nosepokes result in reward delivery and cue presentation. Dotted line represents the

610 active NP. **(b)** Population-averaged trace activity of all recorded D1- (left) and D2- (right) MSNs during

611 cocaine (red/yellow) and sucrose (blue/cyan) self-administration (2 sessions per animal). Dotted lines

612 represent 95% CI of population mean activities generated by shuffling the data 1000x. Yellow and cyan

613 lines represent population-level mean Ca^{2+} activity in cocaine or sucrose trained mice, respectively, outside

614 the 95% CI of the shuffled distribution. **(c)** Heatmaps representing the peristimulus histograms of the mean

615 individual activity of recorded D1- (left) and D2-MSN (right) of mice previously trained on sucrose (upper)

616 or cocaine (lower) around the first 10 cued active nosepoke during PA seeking test, where active nosepokes

617 resulted in cues without any associated rewards. **(d)** Population-averaged trace activity of all recorded D1-

618 (left) and D2- (right) MSNs during cocaine (red/yellow) and sucrose (blue/cyan) PA. Yellow and cyan lines

619 indicate mean Ca^{2+} activity outside the 95% CI. **(e)** Heatmaps representing the peristimulus histograms of

620 the mean individual activity of recorded around the first 10 cued active NP during cued-reinstatement. **(f)**

621 Population-averaged trace activity of all recorded D1- (left) and D2- (right) MSNs during cocaine

622 (red/yellow) and sucrose (blue/cyan) cued-reinstatement. Yellow and cyan lines indicate statistically

623 population-level mean Ca^{2+} activity outside the 95% CI. **(g)** Summary table showing the trends of change

624 of population averaged activity of D1- and D2-MSN in cocaine and sucrose trained animals compared to a

625 randomly generated shuffled distribution (red: increased activity, blue: decreased activity, Grey: no

626 change).

627
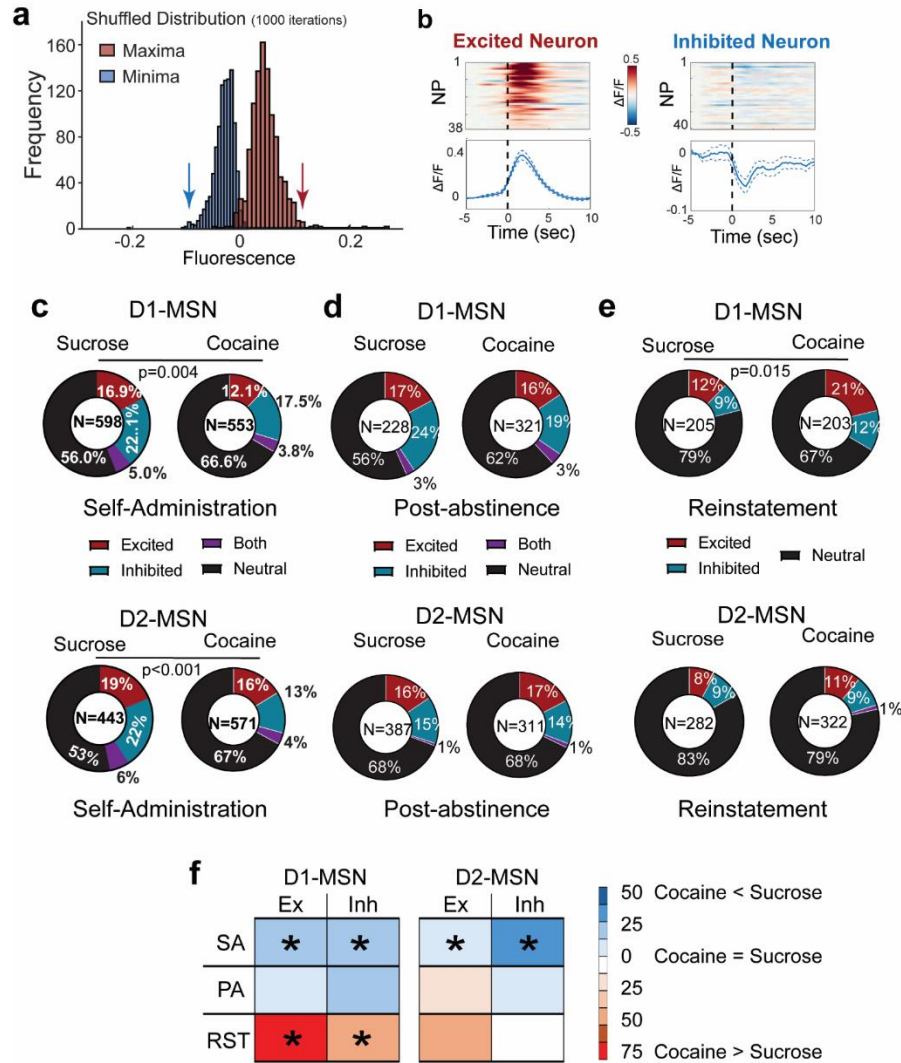
Figure 3. Subpopulations of D1- and D2-MSN time-locked to reward seeking activity

(a) An example of the distribution of the maxima and minima of mean neuronal activity around nosepoke (5 seconds before to 10 seconds after) generated after shuffling the calcium trace of each neuron around behavioral data points (1000x). If the maximum or minimum activity of the real data was higher or lower than 97.5% of the maximum (right) or minimum (left), respectively, the neuron was considered to be time-locked excited or inhibited. Arrows indicate the 97.5% maximum and minimum thresholds. **(b)** Examples of peri-event activity histograms of time-locked excited (left) and time-locked inhibited (right) neurons. Each row of the heatmaps represents an individual trial, i.e. a cued nosepoke. Activity traces in the lower

637   panel represent mean ± SEM activity across all trials. **(c)** Pie charts representing proportions of excited

638   (red) and inhibited (blue) neurons during cocaine or sucrose self-administration show higher proportions of

639   time-locked excited and inhibited neurons in sucrose vs cocaine trained mice. **(d)** Pie charts representing

640   proportions of excited (red) and inhibited (blue) neurons during cocaine or sucrose post-abstinence seeking

641   tests show no difference between both groups. **(e)** Pie charts representing proportions of excited (red) and

642   inhibited (blue) neurons during cocaine or sucrose cued reinstatement seeking tests show no difference

643   between both groups. Cocaine and sucrose were compared using a Chi square test. **(f)** Summary table

644   showing differences in distribution of excited/inhibited timelocked neurons between during different phases

645   of cocaine and sucrose seeking. Coding = %cocaine neurons/ %sucrose neurons within each subpopulation.

646   *$p < 0.05$ based on Chi square test comparing sucrose and cocaine subpopulations within each behavioral

647   trial

648
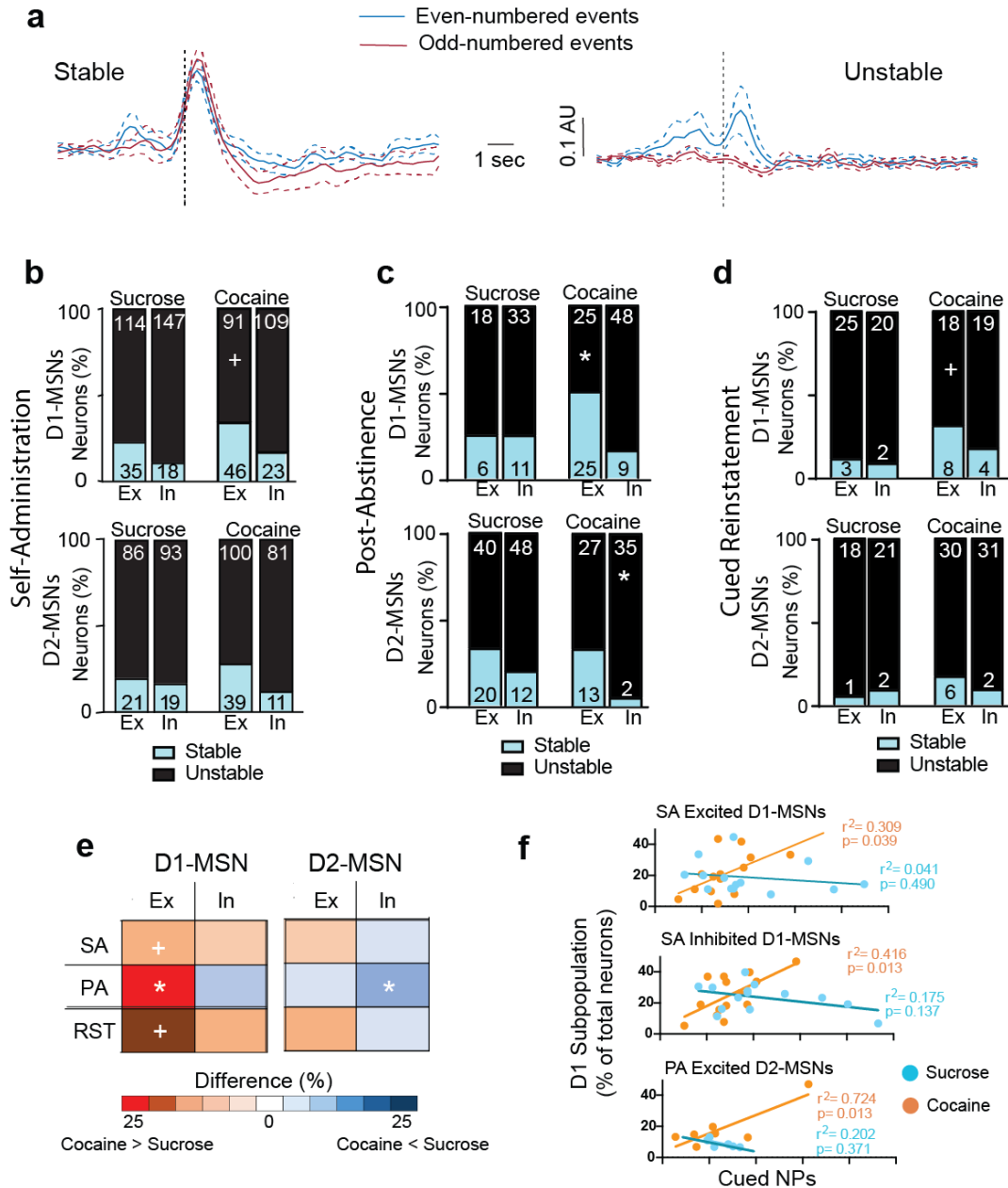
Figure 4. Cocaine seeking is characterized by stable within session excited D1-MSN population.

(a) Example traces of stable and unstable neurons showing respectively consistent and inconsistent mean increase in activity during odd- and even- numbered events. (Red: mean activity around odd-numbered events; blue: mean activity around even numbered events; dotted lines represent the standard error). (b) Bar graphs comparing the stability (blue – stable, black – unstable) of excited (Ex) and inhibited (In) D1-MSN (left) and D2-MSN (right) ensembles during stable self-administration between sucrose- and cocaine-

656   trained animals by comparing time-locking to odd-numbered events to even-numbered events. (* $p < 0.05$

657   cocaine vs sucrose; + $p < 0.10$; see Table S1 for all Chi^2 values). **(c)** Same graph as (b) for post-abstinence

658   test. **(d)** Same graph as (b) for cued-reinstatement. **(e)** Summary table showing percentage of stable neurons

659   within each ensemble during cocaine/sucrose self-administration (SA), post-abstinence seeking (PA), or

660   cued reinstatement (RST). (* $p < 0.05$ comparing ensembles between cocaine sessions and sucrose sessions;

661   + $p < 0.10$; see Table S1 for Chi^2 values). **(f)** Excited D1-MSN significantly predict total number of rewarded

662   and PA NPs in cocaine-trained mice (see Table S2 for r^2 values).
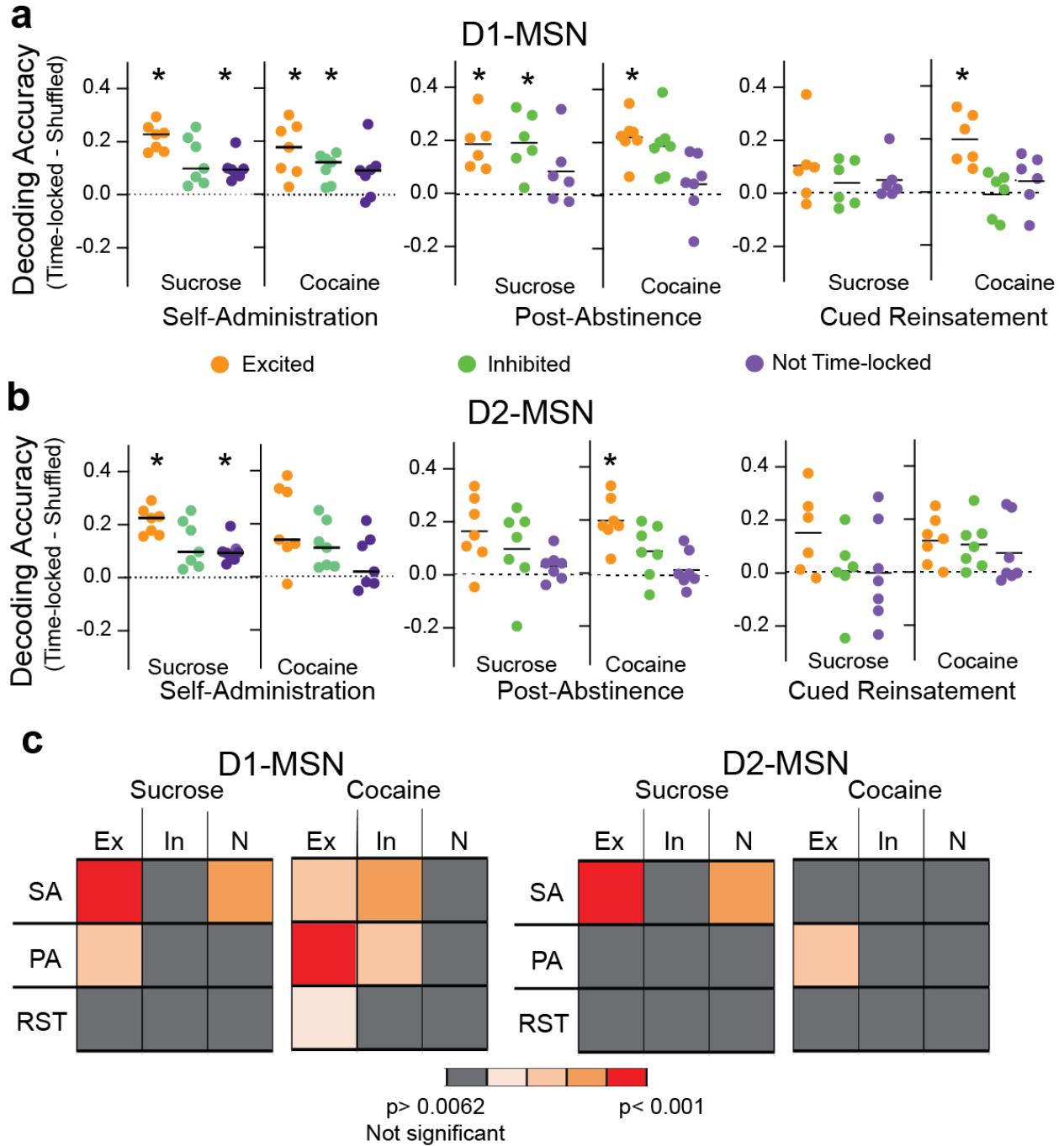
Figure 5. Decoding nose poking by different MSN subpopulations.

(a) Nose poke decoding accuracy using the neuronal data of the three types of D1-MSN activity patterns during self-administration (left), post-abstinence (middle) and cued-reinstatement (right). * p< 0.0062, using a Student's t-test comparing measured data to shuffled data points with the p values corrected for

33

668   multiple comparisons using a false discovery rate, q= 0.02. Table S3 contains all t-test and probability

669   values. **(b)** Nose poke decoding accuracy using the neuronal data of the three types of D2-MSN activity

670   patterns. * p< 0.0062, using a Students t-test comparing measured data to shuffled data points with the p

671   values corrected for multiple comparisons using a false discovery rate of q= 0.02. **(c)** Summary table

672   showing the relative NP decoding accuracy of subtypes of D1- and D2-MSN between sucrose and cocaine

673   trained mice. Ex- excited, In- inhibited, N- not time-locked

674

35
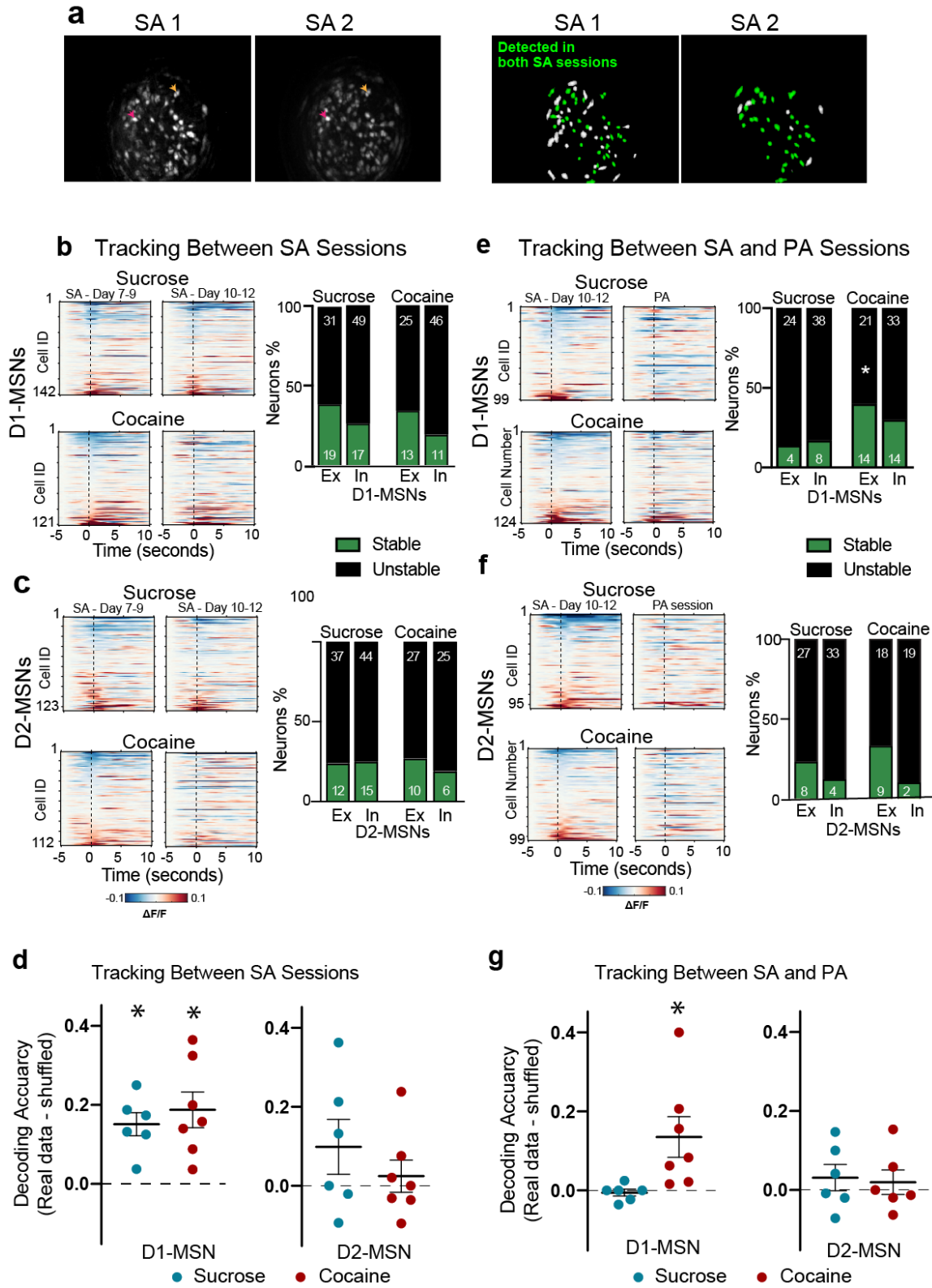
675 **Figure 6. Tracking the same neurons across self-administration (SA) to PA sessions shows a higher**

676 **stability of responding in the excited D1-MSN subpopulation.**

677 **(a)** Left: Maximal intensity projections of recordings from two stable self-administration sessions recorded

678 within the same animal, showing similar fields of view; Right: schematic of the spatial footprints of all

679 identified neurons (green+white) in each session. The neurons that were successfully tracked over both

680 sessions are colored green. The neurons that were only visualized in one session but not the other are colored

681 white. Colored arrows point towards to examples of neurons detected in both sessions. **(b)** Left: Heatmaps

682 representing the mean activity of D1-MSNs longitudinally tracked between two stable cocaine or sucrose

683 self-administration sessions. Each row represents one neuron tracked across both sessions. Right: Bar

684 graphs comparing the stability (green– stable, black– unstable) of excitatory and inhibitory D1-MSNs

685 across two self-administration sessions. **(c)** Heatmaps representing the mean activity of D2-MSNs

686 longitudinally tracked and stability of neuronal activity between two cocaine or sucrose self-administration

687 sessions (SA 8/9 vs SA 10/11). There were no differences in proportion of stable neuron subpopulations

688 between sucrose and cocaine. **(d)** Decoding of the second SA session by training on the first SA session.

689 *$p<0.05$, paired t-test comparing each subpopulation with its shuffled distribution, Table S5 for all t and p

690 values. **(e)** Heatmaps representing the mean activity of D1-MSNs longitudinally tracked and stability of

691 neuronal activity between two cocaine or sucrose SA and PA sessions. Only stable excited D1-MSNs

692 differed between cocaine and saline (Chi^2 and p values in Table S4). **(f)** Heatmaps representing the mean

693 activity of D2-MSNs longitudinally tracked and stability of neuronal activity between cocaine (lower) or

694 sucrose (upper) self-administration (SA 10/11) and PA sessions. No differences between sucrose and

695 cocaine were found (Chi^2 and p values in Table S4). **(g)** Scatter plot showing the decoding accuracy of

696 SVM model trained on the neuronal activity of D1- or D2-MSNs during the SA session and subsequently

697 used to decode NPs during the PA session. Only cocaine D1-MSNs decoded PA NPs (t and p values in

698 Table S5).

Methods

Resource Availability

Lead Contact

Further information and requests for resources and reagents should be directed and will be fulfilled

by the lead contact, Reda M. Chalhoub (chalhoub@musc.edu)

Materials Availability

This study did not generate new unique reagents

Data and code availability

Data reported in this paper, as well as custom MATLAB codes used for the analysis, are available

from the lead contact upon reasonable request.

Any additional information required to reanalyze the data reported in this paper is available

from the lead contact upon request.

Experimental model and subject details

Animals

Adult male and female transgenic D1-cre (129S6.FVB(B6)-Tg(Drd1a-cre)AGsc/KndlJ, Jax Strain

#:028298), D2-cre (B6.129S4(FVB)-Drd2tm1.1Mrub/J, Jax Strain #:010687), and A2A-cre

(B6;129-Adora2atm1Dyj/J, Jax Strain #:010687) mice were used in the experiments. All mice

were bred in-house and periodically outcrossed with wild-type C57/BL/6J mice to maintain

genetic diversity. Mice were group housed before surgeries, and single-housed after surgeries to

avoid interference with behavioral experiments and minimize the risk of infection or injury

resulting from the interaction with cage mates during the recovery period. After surgical

procedures were performed, animals were kept in a reverse light cycle (12-hour dark/12-hour light)

under controlled temperature and humidity settings. All behavioral experiments were run in the

722 Dark Phase. Mice were at least 12 weeks old and weigh 20g prior to their first surgery. All

723 experiments and procedures were performed in compliance with the guidelines of the institutional

724 Animal Care and Use Committee at the Medical University of South Carolina.

Method details

Surgeries

727 All surgical procedures were conducted under isoflurane anesthesia (induction: 5%, maintenance:

728 1-2%, flow rate: 0.2 L/min).

Surgeries for endoscopic calcium imaging

730 After anesthesia induction and preparation and sterilization of the scalp, a small incision was made

731 to expose the skull surface. A dental drill (5mm diameter) was used to create one craniotomy hole

732 over the left nucleus accumbens (AP: +1.6 mm, ML: +1.1 mm relative to Bregma). To achieve

733 cell-type specific calcium imaging, mice were stereotaxically injected with an adeno-associated

734 viral vector encoding a double-floxed inverted orientation GCaMP6f (pAAV-Syn-Flex-

735 GCaMP6f-WPRE-SV40, titer: ~ 1×10^{13} GC/mL, acquired from Addgene (#100833)) using

736 Nanoject III (Drummond Scientific, total volume = 750 nL, rate of injection: 50 nL/min, total

737 duration 10 mins). Four weeks following viral injection, a lens with an integrated baseplate

738 (Inscopix, 0.6 mm diameter, 7.3mm length) was slowly lowered (0.2mm/min) over the same

739 location, under active miniscope visualization and guidance, until a clear and bright plane was

740 visualized, indicating proper expression of the virus and alignment of the lens. The chosen z-plane

741 was constrained to be between -4 and -5 to ensure placement in the nucleus accumbens core. The

742 lens and the baseplate were secured in place using two stainless steel screws (to the skull surface)

743 and dental cement (1:5 mix of black and transparent acrylic cement). The animal's lens was

744 covered with a magnetic cap (Inscopix) to protect it from scratches and physical damage. All mice

745 were weekly monitored through imaging trials over 4 weeks after the surgery to detect single-cell

746 neuronal activity; if no single neurons were visualized, mice were euthanized and excluded from

747 the study.

748 *Catheter Surgeries*

749 For cocaine self-administration in mice, mice were implanted with a custom-made indwelling

750 jugular catheter connected to a back-mounted guide cannula, as previously described[52,53]. In brief,

751 a 12-mm catheter tip was subcutaneously passed from the back and inserted in the right jugular

752 vein through a 1cm mid-scapular incision. The catheter tip was sutured in place to the vein and

753 subcutaneous adipose tissue, while the entry port cannula was secured to the back. All mice

754 received a perioperative analgesic injection of Carprofen (5mg/kg, subcutaneously) and Cefazolin

755 (200 mg/kg, iv) to avoid infections, and were then treated daily with carprofen (5 mg/kg,

756 subcutaneously) and topical antibacterial ointment for 3 days post-operatively. Incision sites were

757 treated with topical triple antibiotic ointment and Catheters were flushed daily with heparin (100

758 units/mL) to prevent catheter occlusion and maintain patency. Patency of the catheters was

759 assessed by injecting the mice with 0.01-0.02mL of Brevital (2mg/mL): an immediate loss of

760 muscle tone within 0-5 seconds following the injection indicated a positive test and a patent

761 catheter. Mice with non-patent catheters at any point during self-administration were excluded,

762 and catheter patency was no longer assessed after the start of home-cage forced abstinence.

763 **Self-administration**

764 After recovering from their respective surgical procedures, mice were switched to a restricted food

765 diet (~3g of chow daily) to maintain their weight at 90% of their original weight. Self-

766   administration was performed in an operative box (Med Associates, Inc) that contains: a house

767   light, two nosepoke ports, an availability light over the active nosepoke, a syringe pump (used for

768   cocaine self-administration), and a sucrose pellet dispenser connected to a tall food pellet

769   receptacle (used during sucrose self-administration).

770   *Sucrose Self-Administration.* Each session started with a 15-minute "baseline" period during which

771   the house light was off and the nosepokes did not result in sucrose delivery, followed by 120-

772   minutes of sucrose self-administration. The "baseline" period was used to adapt the animal to the

773   headcap connections (optical fiber cables for experiments involving optogenetics or miniscope for

774   experiments involving calcium imaging). A maximum of 100 sucrose pellets per session was

775   allowed to prevent an overdose. After self-administration, mice undergo abstinence from sucrose

776   self-administration for 10 days in their home cage during which they were handled daily. After the

777   incubation period, the mice were returned to the operant chamber to undergo a post-abstinence

778   seeking test (PA) during which the active nosepoke resulted in the presentation of the contingent

779   cues associated with the reward, but the sucrose reward was not delivered. After PA testing, mice

780   underwent extinction training to suppress responding to contextual cues. Each extinction session

781   lasted 120 mins (preceded by the 15 mins "light-OFF" period) during which the active nosepoke

782   no longer resulted in the presentation of cues or delivery of the reward. Extinction criteria was

783   determined *a priori* as two consecutive sessions with an average of presses less than 10 nosepokes.

784   At least five extinction training sessions were conducted before the mice underwent reinstatement

785   to the cues. Once the extinction criteria were met, mice underwent a cued-seeking reinstatement

786   test (RST) for 2 hours during which the conditioned cues were returned after every active

787   nosepoke. At the beginning of the reinstatement session, all mice received one free cue at the

788   beginning of the session to elicit operant responding.

789   *Cocaine Self-administration.* After recovery from catheterization surgery, mice were trained daily

790   (1 session/day) to nosepoke the active port to receive a cocaine injection (0.75mg/kg/infusion),

791   which was associated with the presentation of a complex cue (light in the active port and a sound)

792   for 5 seconds, followed by a 20-second time-out period, during which active nosepokes elicited no

793   response. A maximum of 100 cocaine injections per session was allowed to prevent an overdose.

794   Each session started with a 15-minute "baseline" period during which the house light was off and

795   the nosepokes did not result in sucrose delivery, followed by 120-minutes of cocaine self-

796   administration. The "baseline" period was used to collect a baseline recording during the calcium

797   imaging experiments, or to adapt the animal to the headcap connections.

798   Post-Abstinence Seeking Test, Extinction, and Cued Reinstatement. After self-administration,

799   mice undergo abstinence from cocaine self-administration for 7-10 days in their home cage during

800   which they were handled daily. After the incubation period, the mice were returned to the operant

801   chamber to undergo a post-abstinence seeking test (PA) for 120 minutes (preceded by the 15 mins

802   "light-OFF" period) during which the active nosepoke resulted in the presentation of the contingent

803   cues associated with the reward, but the cocaine reward was not delivered. For experiments

804   including optogenetic and chemogenetic manipulations, multiple PA seeking tests were performed

805   to assess persistence of the behavioral responses. After PA testing, mice underwent extinction

806   training to suppress responding to contextual cues. Each extinction session lasted 120 mins

807   (preceded by the 15 mins "light-OFF" period) during which the active nosepoke no longer resulted

808   in the presentation of cues or delivery of the reward. Extinction criterion was determined *a priori*

809   as two consecutive sessions with an average less than 10 nosepokes. At least five extinction

810   training sessions were conducted before the mice underwent reinstatement to the cues. Once the

811   extinction criterion was met, mice underwent a cued-seeking reinstatement test (RST) for 2 hours

41

812   during which the conditioned cues were returned after every active nosepoke. At the beginning of

813   the reinstatement session, all mice received one free cue at the beginning of the session to elicit

814   operant responding. Mice were considered successfully reinstated in response to the cue if they

815   nosepoke for the cue >10 times during a single session. Mice that failed a reinstatement test were

816   given 1 more day of extinction before repeating the reinstatement test. Mice that failed two cued-

817   reinstatement tests were excluded from the reinstatement test analysis.

818   **Calcium Imaging from freely behaving animals**

819   *Acquisition*. We recorded calcium activity of D1- and D2-MSN in freely behaving D1- and

820   D2/A2A-cre mice respectively using miniature fluorescent microscopes "miniscopes" (nVista 3.0,

821   Inscopix) on intermittent non-consecutive days throughout self-administration, post-abstinence

822   seeking test, extinction training and reinstatement sessions. After the lens placement surgery,

823   calcium dynamics were monitored weekly until individual neuron calcium changes were detected.

824   These sessions were also used to adapt the mice for the weight of the miniscope. These mice were

825   then randomized into cocaine self-administration and sucrose self-administration groups. Before

826   the beginning of the first recording session, the gain (limit 2-4), the LED intensity (0.5-1

827   mW/mm^2), and the desired z-plane were optimized per animal to obtain the highest number of

828   well-defined regions of interests (ROIs), or putative neurons. The gain and LED settings were

829   saved to be used in all subsequent sessions; the z-plane was electronically adjusted to match the

830   same field of view during every session to allow tracking of the same neurons across time. All

831   recordings were performed at 15 Hz (exposure time = 0.667 seconds), at 2x spatial down-sampling

832   rate to reduce the generated file size. The operant chambers were connected to the Inscopix Data

833   Acquisition Box using two transistor-transistor logic (TTL) via BNC cables to synchronize the

834   recorded calcium imaging frames and behavioral events.

Image Processing and Signal Extraction

Processing and ROI segmentation. The pre-processing and ROI segmentation were performed using the MATLAB application programming interface (API) of Inscopix Data Processing Software v1.6 or custom MATLAB codes. The generated recordings were spatially down-sampled (2x in both dimensions) to reduce the file size and allow shorter processing times. Any defective pixels or dropped frames were corrected by linear interpolation from nearby pixels and frames. A spatial bandpass filer (0.005-0.5 pixels-1) was next applied to remove the low and high spatial frequency components that do not correspond to cells in focus. This was followed by applying a frame-by-frame motion correction algorithm to account for any motion artifacts. The signal was then normalized to background by subtracting and dividing each pixel value by the mean intensity of that pixel over the entire recording, as follow:

$\Delta F/F\_0 = (F-F\_0)/F\_0$, where F_0 = pixel intensity at mean frame

A principal component analysis (PCA), followed by an independent component analysis (ICA), were used to segment the recording into independent spatial footprints of putative neurons. The corresponding temporal trace of each spatial footprint was calculated by applying the spatial footprint on the background normalized movie. All components were manually inspected and included in the analysis if they show typical neuronal shape of the spatial footprints and canonical calcium signals of their corresponding temporal trace. If two neighboring neurons (distance<5 pixels) have highly correlated temporal traces (coefficient>0.9), the neuron with the lower signal-to-noise ratio (SNR) is excluded from the analysis to eliminate any duplicate components belonging to the same neuron.

43

856   Detection of Excitatory Calcium Events. Ca2+ excitatory events were detected using Inscopix Data

857   Processing Software whenever the amplitude of the temporal trace crossed a 6 median absolute

858   deviation (MAD), with an indicator decay time of 200ms. The time of the Ca2+ event occurrence

859   was determined as the start of the event.

860   **Histology**

861   At the end of the behavioral experiments, the animals were deeply anesthetized with isoflurane

862   and then transcardially perfused with 10mL of phosphate buffer-saline (PBS) followed by 20mL

863   of 10% formalin solution. The brains were extracted and fixed in 10% formalin solution overnight

864   and then transferred to 20% sucrose in PBS for cryoprotection. After 24 hours, the brains were

865   frozen in dry ice and cut into 40μm sections using a cryostat. For immunohistochemical staining,

866   free-floating sections were blocked with 2% normal donkey serum in 2% PBST for 1 hour on a

867   shaker at room temperature. These sections were incubated overnight at 4ºC in blocking solution

868   containing chicken anti-GFP antibody (1:1000, Abcam ab13970). The next day, the sections were

869   washed 3x for 5-minutes with 0.1% PBST solution, before staining them with standard Alexa

870   conjugated secondary antibody (488 Goat Anti-Chicken, Thermofischer scientific: A-11039) for

871   2 hours. Hoechst 33258 (1:2000, Thermofischer) was added to slides during the last 15 minutes of

872   incubation with secondary antibody to stain for nuclei. Finally, brain sections were washed,

873   mounted on glass slides, and cover-slipped after adding Prolong Fold Fluorescent mounting

874   medium. To ensure successful virus expression and accurate lens placement, confirmation was

875   conducted following the staining under fluorescent microscopy.

876   **Quantification and statistical analysis**

877   **Calcium Imaging Analysis**

878 *Time-locked neurons.* Time-locked neurons were defined similarly to what was previously done[54].

879 Briefly, the actual calcium activity of all neurons around the active nosepokes (-5s before to 10s

880 after) was extracted, aligned to nosepoke onset, and averaged over the number of trials of interest

881 (all or first 10 nosepokes). For every neuron, the Ca^{2+} activity around each rewarded nosepoke was

882 normalized to a baseline taken between -5 to -3 seconds before the nosepoke. The averaged 15-

883 second fluorescent neurons across the first 10 nosepokes were used to plot the peri-stimulus

884 heatmaps for the represented sessions. The average trace of all neurons was compared to a 1000x

885 shuffled distribution of means, obtained by circularly shuffling the calcium trace with respect to

886 the nosepoke timestamps 1000x and generating a null distribution of peri-stimulus histograms.

887 95% confidence intervals of the null distribution are plotted to compare to the trace generated from

888 real data.

889 To test whether a neuron was time-locked inhibited or time-locked excited, the maximum and

890 minimum mean activity of each neuron was compared to a shuffled distribution of 1000 maxima

891 and 1000 minima expected by chance. The shuffled distribution was generated by circularly

892 shuffling the temporal trace of every neuron around the behavioral events by random values and

893 calculating the minimum and maximum random mean activity at every iteration. A neuron was

894 considered significantly inhibited if its actual minimum was lower than the 2.5th percentile of the

895 shuffled distribution of minima, and significantly excited if its actual maximum was higher than

896 the 97.5th percentile of the shuffled distribution of maxima.

897 The stability of the time-locked neurons within the same session was assessed by using odd-

898 numbered events and even-numbered events. The neurons determined to be time-locked with

899 similar activity patterns (excited or inhibited) to both sets were considered stable. All events were

900 used in these analyses. Second, we repeated the time-locked analysis using the first 10 rewarded

45

901 nosepokes and the second 10 rewarded nosepokes. The neurons determined to be time-locked with

902 similar activity patterns to both sets were considered stable.

903 *Tracking neurons across different sessions*. Neurons between multiple sessions were tracked using

904 a previously established nearest-neighbor cell registration method[19,55]. Maximum intensity

905 projections for each session were generated and thresholded at 50% of the maximum pixel value,

906 and the generated FOVs between sessions were first aligned to a reference session (last session of

907 self-administration), using translational corrections only. A threshold for a candidate cell to be

908 used for registration was determined by calculating within-session distances between nearest

909 neighbors. Nearest neighbor centroid distances were found to be always greater than 4µm; we

910 chose 3µm as a threshold to further reduce the chance of incorrect cross-session registration.

911 Neurons were tracked between two late self-administration sessions. Neurons were also tracked

912 between either of the two recorded self-administration sessions and the post-abstinence session:

913 the pairing resulting in a higher number of tracked neurons was selected for analysis to maximize

914 the power of the analyses.

915 *Decoding Analysis*. The nosepokes and cues were decoded using support vector machine models

916 trained on the neural data 5 second before or 5 second after the nosepoke occurrence, respectively.

917 For every event, a matched non-event epoch was randomly selected from the session, such as it is

918 30 seconds separated from any behavioral event in the session. Four-fold cross-validation was used

919 to evaluate the ability of the model to decode the validation set. After the four iterations, a mean

920 decoding accuracy is calculated and used to assess the ability of the neuronal data to predict the

921 behavioral events. The labels of the events and non-events were shuffled to generate the shuffled

922 distribution. For ensemble decoding, the ensembles were selected based on time-locked activity

923 across all events. All decoding accuracy scores were compared between animals using 2-way

46

924 ANOVA, followed by Bonferroni correction. For decoding analysis in longitudinally tracked

925 neurons, an SVM model was trained using all the data from one session (SA), the resultant model

926 was then applied to a test data from the test session (SA or PA). The performance of all models

927 were compared to models trained on neuronal with shuffled event labels. Data was plotted and

928 reported as decoding accuracy using the real data subtracted from the decoding accuracy when

929 using the shuffled dataset.

Statistical Analysis and Graphics

930

931 Heatmaps and example traces were generated using MATLAB. Summary graphical

932 representations were generated using GraphPad Prism v9. All statistical analysis were performed

933 using either MATLAB 2022b or GraphPad Prism v9. All statistical rests were corrected for

934 multiple comparisons with the Bonferroni method when applicable. Comparisons of fractions of

935 neurons were done using Chi-Square tests. For the decoding results, all comparisons were made

936 using paired Student's t-tests (real vs shuffled) and p values were corrected using a false discovery

937 rate with q=0.02. Animals in which there was <10 neurons were excluded from the analyses but

938 included in the behavioral data in figure 1. For all analysis, a p-value of 0.05 was considered

939 significant a priori.